Article

Chinese Science Bulletin

Oceanology

May 2013 Vol.58 No.15: 1832–1837
doi: 10.1007/s11434-012-5576-2

Solar forced transient evolution of Pacific upper water thermal structure during the Holocene in an earth system model of intermediate complexity

WANG Yue[1*], JIAN ZhiMin[1], ZHAO Ping[2,3], DANG HaoWen[1] & XIAO Dong[3]

[1] *State Key Laboratory of Marine Geology, Tongji University, Shanghai 200092, China;*
[2] *National Meteorological Information Center, Beijing 100081, China;*
[3] *Institute of Climate System, Chinese Academy of Meteorological Sciences, Beijing 100081, China*

Received August 17, 2012; accepted October 16, 2012; published online December 13, 2012

Forced by transient solar activities since 7 ka, the thermal structures of the Pacific upper water at boreal winter are featured by an enhanced response of 3-dimensional Western Pacific Warm Pool (WPWP) in an Earth system model of Intermediate Complexity at centennial scales. During solar maximum periods, the magnitude of surface ocean temperature variations is 30% larger in the western tropical Pacific than in the Niño3 region, while at subsurface, it is 40% larger in the subtropical North Pacific than in the western Equatorial Pacific. They compromise stronger zonal and meridional thermal gradients in surface and subsurface Pacific respectively which are both linearly responded to solar forcing at centennial periods. The surface gradient is most sensitive at 208-year period while the subsurface gradient shows more significance at periods longer than 208-year. Also noteworthy are two differences: (1) the phase lags at these periods of surface gradient are slightly smaller than that of subsurface; (2) the 148-year and 102-year periods in surface gradient are lost in subsurface gradient. These modeled features preliminary confirm the centennial fluctuations of WPWP in paleo-proxies and a potential solar forcing during the Holocene.

solar activities, upper water structure, Western Pacific Warm Pool, paleoceanographic simulation, centennial fluctuations

Citation: Wang Y, Jian Z M, Zhao P, et al. Solar forced transient evolution of Pacific upper water thermal structure during the Holocene in an earth system model of intermediate complexity. Chin Sci Bull, 2013, 58: 1832–1837, doi: 10.1007/s11434-012-5576-2

Modern climate studies have shown that, small-magnitude variations of Total Solar Irradiance (TSI) at the top of atmosphere (TOA) can induce significant surface climate responses at decadal and interdecadal time scales [1,2]. For example, Clement et al. [3] proposed that uniform heating over the entire tropical region will warm the Pacific more in the west than in the east and strengthen the zonal equatorial Sea surface temperature (SST) gradient. So the Pacific upper water thermal structure may act as a transmitter of solar forcing with a La Nina-like SST pattern in Pacific during solar maxima periods [4,5].

Since the Holocene is featured by significant millennial-centennial fluctuations of solar activities [6], there are a growing number of paleoclimatic studies pointing toward a stronger solar forcing on past climate [7–11]. The enhanced response of the Western Pacific Warm Pool (WPWP) is first recorded in surface temperature anomalies between the Medieval and the Little Ice Age [12]. The centennial zonal oscillations of Pacific SST forced by solar activities are also significant in the Mg/Ca records of early Holocene [13] and supported by a transient Holocene simulation of the El Niño-Southern Oscillation (ENSO) [14]. However, this simulation used a simple Zebiak-Cane (ZC) model constrained in tropical Pacific and it is still unknown whether their results are independent of model.

And more, it has been shown High TSI at periods of 11-year and 22-year can induce 0.03 and 0.06 K warming of the subsurface water at 80–160 m depth (i.e. Thermocline Water Temperature, TWT) [15,16]. Though these adjustments of upper water structures in tropical Pacific may be

*Corresponding author (email: 163wangyue@163.com)

linked with the ENSO-like SST pattern, little attention has been paid to the spatial-temporal variations of TWT forced by centennial solar activities during the Holocene.

Here in an Earth system Model of Intermediate Complexity (EMIC) with transient accelerated TSI forcing since 7 ka, enhanced responses of WPWP are simulated with different spatial/spectrum patterns of SST and TWT at centennial periods, and their meanings for paleoclimate are interpreted with multi-proxies of paleoceanography.

1 Model, experiment and data processing

The model used here is the University of Victoria Earth System Climate Model, Version 2.9 (UVic_ESCM), which employs a 3.6°×1.8° horizontal resolution and 19 vertical levels for the ocean. This 3-D ocean general circulation model is coupled to a 2-D energy-moisture balance atmospheric model with dynamical feedbacks, a dynamic-thermodynamic sea-ice model and a land surface scheme. To isolate the thermal response of Pacific upper water from internal variability, the atmospheric dynamical feedback option (which may damp the "ocean thermostat" mechanism [3]) has not been included in this application and the model uses prescribed present-day winds in its climatology. Weaver et al. [17] further described the model version (including the atmospheric, Ocean and sea ice model), its ability in reproducing the observed Pacific SST/TWT structures, and its sensitivity to transient solar forcing in global warming experiments.

For our transient accelerated experiment (Exp_{solar}), we started from the TSI at 9.3 ka [6] and advanced it by 10 years at the end of each model year (acceleration factor = 10). The model was integrated for 930 model years with its original configurations except for this transient forcing. It means that other boundary conditions were kept constant at modern values (including orbital parameters). This acceleration technique has been used to reveal the transient behaviors of summer monsoon in fully coupled general circulation models (GCMs) at orbital timescales [18–20]. And the effects of different acceleration factors can be neglected for the external forcing that vary on (centennial) timescales longer than the actual length of the model response [21,22]. To diminish the uncertainties due to initial state, the first 230 model years were abdicated as adjustments for atmosphere-upper ocean system since the Pacific SST and TWT (−120 m water depth) both reached equilibrium during the last 700 model years (7 to 0 ka) (Figure 1(a)).

Since modern Pacific upper water changes are most significant at boreal winter, we first calculated December-January-February (DJF) SST anomalies and TWT anomalies

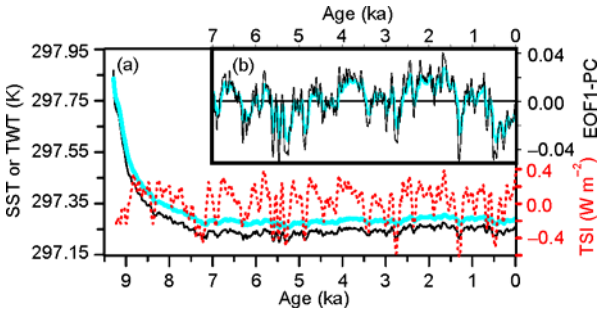

Figure 1 In (a), the detrended TSI anomalies (red dashed line, 9-points smoothed) (Units: W m^{-2}) [6] are shown together with timeseries of annual averaged tropical (30°S to 30°N) SST (black thin line) and TWT (blue thick line, added by 4.2 K for comparison); In (b), EOF1-PCs of SST (black thin line, multiplied by −1) and TWT (blue thick line) both can be matched well with the TSI evolution.

from the monthly results (the last 700 model years) of Exp_{solar}. Then an unrotated Empirical Orthogonal Functions (EOF) analysis with area weighting was used to extract the main spatial modes (Figure 2) and temporal evolutions (Principal components, PCs in Figure 1(b)) of DJF SST (TWT) anomalies. Based on the definitions in Figure 2(a), we calculated the regional averaged timeseries of DJF SST anomalies in WPWP and Niño3 region respectively and differenced them as a zonal (WPWP-Niño3) SST gradient timeseries (Figure 3(a)). Similarly, a meridional TWT gradient was calculated between subtropical North Pacific (NPac) and Western Equatorial Pacific (WEP) defined in Figure 3(b). Finally, a cross-spectrum analysis using the NCAR command Language (NCL)[1)] was conducted between the SST (TWT) gradient and TSI forcing to reveal

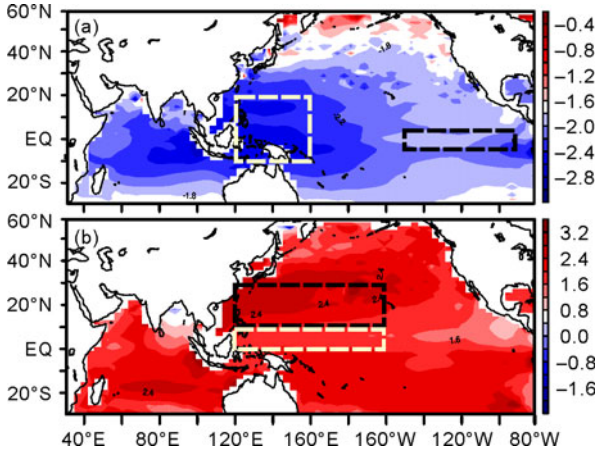

Figure 2 (a) and (b) show the EOF1 spatial modes of DJF SST and TWT respectively. The rectangles in (a) and (b) denote the boundaries of regions: WPWP (10°S–20°N/120°–160°E), Niño3 (5°S–5°N/150°–90°W), WEP (0°–10°N/120°E–160°W), and NPac (10°–30°N/120°E–160°W).

1) The NCAR Command Language (Version 6.0.0) [Software]. (2012). Boulder, Colorado: UCAR/NCAR/CISL/VETS. http://dx.doi.org/10.5065/D6WD3XH5.

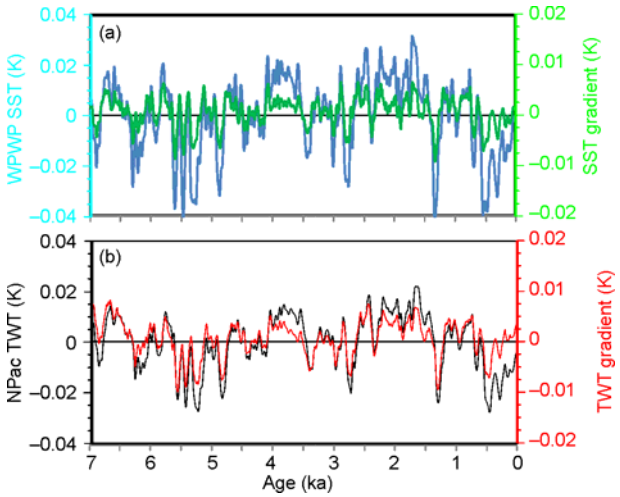

Figure 3 Regional averaged timeseries of DJF SST anomalies in WPWP (blue line) (Units: K) is shown in (a) with its differences (green line) relative to SST timeseries in Niño3 region; while regional averaged timeseries of TWT anomalies in NPac (black line) is shown in (b) with its differences (red line) relative to TWT timeseries in WEP region.

their phase relationship at different centennial periods (Figure 4), which were compared with the spectrum of Mg/Ca SST/TWT and other paleorecords in WPWP (Figure 4(d)–(f) and Figure 5). Here the spectrums of Paleorecords are cal culated by the REDFIT software [23] using rectangle-type window. Since our simulation excluded transient variations of orbital parameters, all the timeseries used for comparison here were first detrended by 4-order polynomial fitting method.

2 Results and discussion

2.1 Solar forced SST and TWT responses in Pacific

To reveal the TSI forced upper water thermal evolutions, the EOF results based on DJF SST and TWT are shown in Figure 1(b) and Figure 2. The first EOF "spatial" modes (EOF1) of SST and TWT (Figure 2) account for 91.0% and 77.4% of the total variance respectively and both show centennial variations in their PCs (Figure 1(b)). Noteworthy are their different spatial patterns: the SST shows larger magnitudes (30%) in WPWP (−2.4) than in the Niño3 region (−1.6) (Figure 2(a)), while the TWT changes in NPac (2.2) are enhanced by 40% relative to WEP (1.6) (Figure 2(b)). Interestingly, these spatial patterns are similar to the climatological distributions of WPWP temperature at 0 and −120 m water depth [24] respectively. And the TWT patterns can further represent the distributions of thermocline depth or upper ocean heat content [15,25] in WPWP. In short, inhomogeneous responses of Pacific upper water are induced by centennial solar fluctuations during the Holocene, indicating an enhanced response of 3-D WPWP with a zonal SST gradient and a meridional TWT gradient.

Note that the signs of EOF results only indicate relative positive/negative phases, the EOF1 PCs of SST and TWT are linearly respond to the Holocene TSI forcing (Figure 1). Similar linear responses also prevail in the timeseries of regional averaged SST/TWT and their gradients (Figure 3). Due to the increased TSI at TOA (1 W m^{-2} from TSI_{min} to TSI_{max}), the WPWP SST and the NPac TWT exhibit a warming of 0.04–0.07 K and 0.02–0.04 K respectively, while the zonal SST gradient and meridional TWT gradient are both increased by 0.02 K (Figure 3) which are consistent with previous studies [15,16]. Despite of these differential magnitudes, more meaningful are their spectrum features.

In the frequency spectrum of TSI, periods of 102, 142, 208, and 357 years are most significant at 90% confidences and the periods of 500, 769 and 1100 years are also clearly resolved (Figure 4(a)). The periods of 90% significance are linearly transferred to the spectrum of the zonal SST gradient (black line in Figure 4(b)) with the strongest magnitudes at periods of 208 years while the periods of 769 and 500 years are significant at 80% level. In spectrum of TWT gradient (black line in Figure 4(c)), the magnitudes at periods of 208, 142 and 102 years are greatly suppressed but are still significant at 90% level with other centennial periods. Considering the cross spectrum (blue and purple lines in Figure 4(b)), zonal SST gradient is highly correlated with TSI at periods of 1100, 769, 500, 357, 208, 142 and 102 years and shows phase (time) lags of 15° (46 years), 15° (32 years), 15° (21 years), 25° (25 years), 50° (29 years), 60° (24 years), 70° (20 years) (SST gradient lags TSI). In contrast, peaks of 142 and 102 years are missed in TWT gradient (blue line in Figure 4(c)), and larger phase lags against TSI (20° (61 years), 20° (43 years), 30° (42 years), 50° (50 years) and 80° (46 years)) appear for periods of 1100, 769, 500, 357, 208 years. It seems that these phase lags are decreased at longer timescales for both two gradients, and can be converted to an averaged time lag (or response time) of 28 (48) years for SST (TWT) relative to centennial TSI forcing respectively. This longer response time of TWT and the lack of high frequency can be attributed to the "low-pass filter" effect of the upper ocean.

With a warmer WPWP at surface, the stronger zonal SST gradient agrees well with the "ocean thermostat" hypothesis [3] and may indicate a solar forced ENSO-like response [14] at centennial scales. Further, the enhanced meridional TWT gradient is reversed with a meridional SST gradient (with warmer WPWP and relative cooler SST north of 30°N) in Western Pacific (Figure 2(a)). Since the equatorial thermocline water is mainly sourced from the subduction and advection of midlatitude waters [26], and considering the thermal effect on water density, there may be more subduction at 30°N and a stronger meridional Subtropical Thermocline Circulation (STC) in Pacific [27,28]. This STC and the surface ENSO commonly alter the operation of ocean thermostat centered with an enhanced 3-D WPWP. Considering the simplicity of the model, our discussion will be limited on the Pacific upper water thermal variations while the detailed

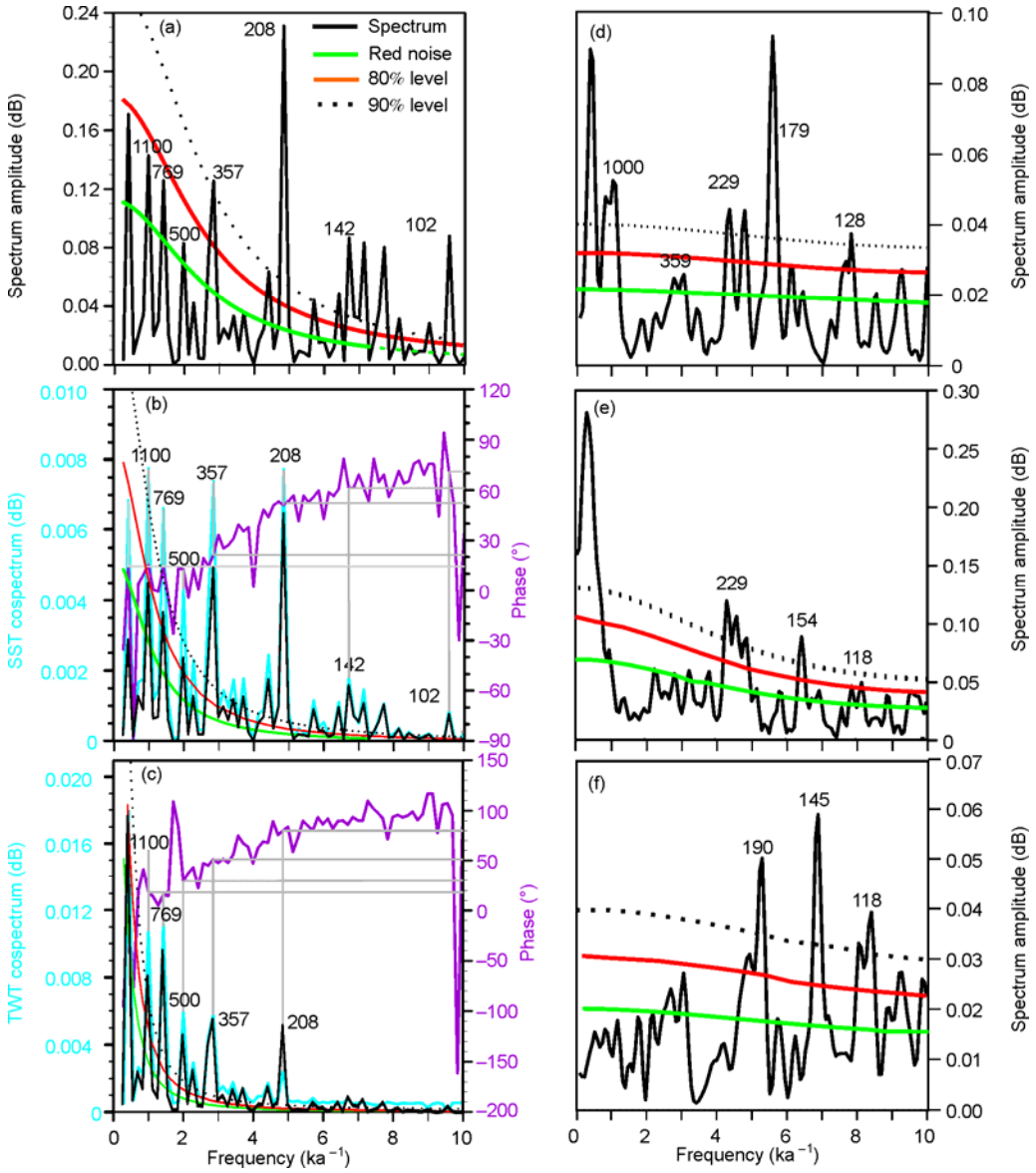

Figure 4 The spectrum of TSI (unsmoothed), SST gradient, TWT gradient, the Mg/Ca SST of MD98-2176, MD98-2181 and 13GGC are shown as the black peaks in (a)–(f) which are calculated by the REDFIT software [23]. Additionally, the cross-spectrum between TSI and SST gradient are shown as power magnitudes (blue line) and phase angles (purple line) against TSI in (b); (c) is similar to (b) but for the situations of TWT gradient.

evolution of STC and ENSO should be accessed in EMICs or CGCMs with dynamical atmospheric feedbacks [29].

2.2 Drawbacks and comparisons with proxy-records of paleoceanography

Several limitations constrain the detailed comparisons between our simulation and the paleorecords of Pacific SST/TWT: (1) with great uncertainties, the magnitude of TSI is roughly a factor of 10–100 smaller than other forcing (volcano, orbital insolation, greenhouse gases) in paleoclimate and our solar forced SST/TWT variations may be covered up by them; (2) As an EMIC, our coarse resolution model is limited in physical processes (i.e. atmospheric feedbacks, especially from stratosphere) for a realistic simulation of past climate. But it is still suitable for testing the sensitivities of upper water column to solar forcing that may be underestimated by CGCMs, because the "thermostat" mechanism is dampened by atmospheric effects in CGCMs [12,30]. Despite of those discrepancies, here we only focus on the common spectrum features.

In the ZC model [14], a zonal SST gradient linearly responds to TSI forcing and shows a short phase lag (about a decade) at periods of 200–500 and 800–1000 years. Similar periods appear in Mg/Ca-SST record of Northeast Pacific with 50–100 years' lag [13] and can be comparable with our SST results (Figure 4(b)). Centennial SST changes are also found in Holocene proxy-records from the western Philippine

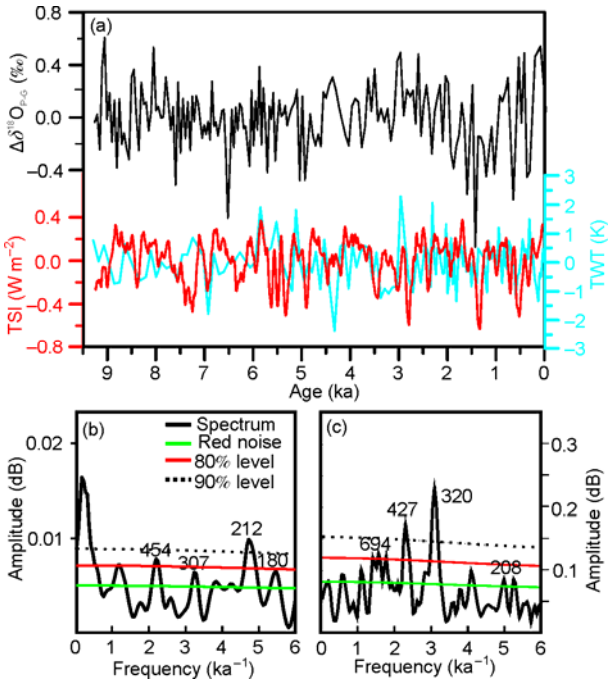

Figure 5 (a) Detrended timeseries of MD01-2386 $\Delta\delta^{18}O_{P\text{-}G}$ (black line) and MD98-2188 Mg/Ca TWT (blue line) are compared with the TSI anomalies (9-points smoothed) (red line); (b) and (c) show the spectrum of MD01-2386 $\Delta\delta^{18}O_{P\text{-}G}$ and MD98-2188 Mg/Ca TWT respectively.

Sea (MD98-2188) [31], Makassar Strait (13GGC) [32], Mindanao Sea (MD98-2181) and Flores Sea (MD98-2176) [33]. All of their spectrums are significant at centennial periods (especially 190–229 years) of solar cycle (Figure 4(d)–(f)). But due to uncertainties in their age models, resolutions, local environments and other forcing factors, it is difficult to fully match these quasi-period bands with those of solar forcing and to compare their phase angles as shown in Figure 4(b).

Besides these surface variations, multi-proxies of paleoceanography have revealed centennial fluctuations of thermocline water in WPWP. For example, the thermocline depths indicated by $\Delta\delta^{18}O_{P\text{-}G}$ records (black line in Figure 5(a)) during the Holocene show significant 212-year periods (Figure 5(b)) in WEP (MD01-2386) [34][2)]. More direct evidences can be found in the Mg/Ca-TWT records from western tropical Pacific (MD98-2188) [31]: the TWT timeseries share similar variability with detrended TSI during 6.9, 4.3–3.4, and 3–0.3 ka (Figure 5(a)) and show centennial periods of 320, 427 and 694 years (Figure 5(c)). Again, shorter periods of TWT are suppressed (208 years) as our simulation. So our simulated TWT results can be used to argue for a possible solar origin of these paleoceanographic variations.

3 Conclusions

Forced by the transient TSI forcing since 7 ka, the inhomogeneous evolution of Pacific upper water structures in an EMIC is featured by an enhanced thermal response of 3-dimensional WPWP at centennial scales. At surface, the magnitude of SST variations in the WPWP is larger than that of EEP, and results in a stronger zonal SST gradient in tropical Pacific during TSI_{max} intervals. While at subsurface, the magnitude of TWT shows larger responses in the subtropical North Pacific than in the WEP regions and induces a stronger meridional TWT gradient. These two gradients both exhibit high correlation to TSI fluctuations at periods of 1100, 769, 500, 357 and 208 years with smaller phase lags (relative to TSI forcing) at longer timescales. And the phase lags of SST gradient at these periods are smaller than those of TWT gradient. Confirmed by paleorecords from WPWP, the most significant periods in SST gradient are weakened (208 years) or disappeared (148 and 102 years) in TWT gradient. These transient thermal features, which may indicate the solar forced Pacific upper water changes over the last 7 ka, should be further accessed in models with improved physics and higher resolutions or in comparison with more proxy-records of paleoceanography.

This work was supported by the National Basic Research Program of China (2007CB815901) and the National Natural Science Foundation of China (41023004 and 91028004). We thank Chinese Academy of Meteorological Sciences for providing computing resources and technical support. We should also thank the improvements and comments from three anonymous reviewers.

1 Gray L J, Beer J, Geller M, et al. Solar influences on climate. Rev Geophys, 2010, 48: RG4001
2 Lean J L. Cycles and trends in solar irradiance and climate. Wiley Interdiscip Rev Clim Change, 2010, 1: 111–122
3 Clement A C, Seager R, Cane M A, et al. An ocean dynamical thermostat. J Clim, 1996, 9: 2190–2196
4 Meehl G A, Arblaster J M, Matthes K, et al. Amplifying the Pacific climate system response to a small 11-year solar cycle forcing. Science, 2009, 325: 1114–1118
5 Meehl G A, Arblaster J M. A lagged warm event-like response to peaks in solar forcing in the Pacific region. J Clim, 2009, 22: 3647–3660
6 Steinhilber F, Beer J, Frohlich C. Total solar irradiance during the Holocene. Geophys Res Lett, 2009, 36: L19704
7 Bond G, Kromer B, Beer J, et al. Persistent solar influence on North Atlantic climate during the Holocene. Science, 2001, 294: 2130–2136
8 Fleitmann D, Burns S J, Mudelsee M, et al. Holocene forcing of the Indian monsoon recorded in a stalagmite from Southern Oman. Science, 2003, 300: 1737–1739
9 Neff U, Burns S J, Mangini A, et al. Strong coherence between solar variability and the monsoon in Oman between 9 and 6 kyr ago. Nature, 2001, 411: 290–293
10 Clemens S C. Millennial-band climate spectrum resolved and linked to centennial-scale solar cycles. Quat Sci Rev, 2005, 24: 521–531

2) The $\Delta\delta^{18}O_{P\text{-}G}$ data used here was its high resolution version (unpublished) provided by our coauthor Jian Zhimin.

11 Mann M E, Cane M A, Zebiak S E, et al. Volcanic and solar forcing of the tropical Pacific over the past 1000 years. J Clim, 2005, 18: 447–456
12 Mann M E, Zhang Z H, Rutherford S, et al. Global signatures and dynamical origins of the Little Ice Age and Medieval climate anomaly. Science, 2009, 326: 1256–1260
13 Marchitto T M, Muscheler R, Ortiz J D, et al. Dynamical response of the tropical Pacific ocean to solar forcing during the early Holocene. Science, 2010, 330: 1378–1381
14 Emile-Geay J, Cane M, Seager R, et al. El Niño as a mediator of the solar influence on climate. Paleoceanography, 2007, 22: PA3210
15 White W B, Lean J, Cayan D R, et al. Response of global upper ocean temperature to changing solar irradiance. J Geophys Res [Oceans], 1997, 102: 3255–3266
16 White W B, Cayan D R, Lean J. Global upper ocean heat storage response to radiative forcing from changing solar irradiance and increasing greenhouse gas/aerosol concentrations. J Geophys Res [Oceans], 1998, 103: 21355–21366
17 Weaver A J, Eby M, Wiebe E C, et al. The UVic earth system climate model: Model description, climatology, and applications to past, present and future climates. Atmos Ocean, 2001, 39: 361–428
18 Kutzbach J E, Liu X D, Liu Z Y, et al. Simulation of the evolutionary response of global summer monsoons to orbital forcing over the past 280000 years. Clim Dyn, 2008, 30: 567–579
19 Chen G S, Liu Z Y, Clemens S C, et al. Modeling the time-dependent response of the Asian summer monsoon to obliquity forcing in a coupled GCM: A PHASEMAP sensitivity experiment. Clim Dyn, 2011, 36: 695–710
20 Wang Y, Jian Z, Zhao P. Extratropical modulation on Asian summer monsoon at precessional bands. Geophys Res Lett, 2012, 39: L14803
21 Lorenz S J, Lohmann G. Acceleration technique for Milankovitch type forcing in a coupled atmosphere-ocean circulation model: Method and application for the holocene. Clim Dyn, 2004, 23: 727–743
22 Timm O, Timmermann A. Simulation of the last 21000 years using accelerated transient boundary conditions. J Clim, 2007, 20: 4377–4401
23 Schulz M, Mudelsee M. REDFIT: Estimating red-noise spectra directly from unevenly spaced paleoclimatic time series. Comput Geosci, 2002, 28: 421–426
24 Locarnini R A, Mishonov A V, Antonov J I, et al. World Ocean Atlas 2005, Volume 1: Temperature. In: Levitus S, ed. NOAA Atlas NESDIS 61. Washington D C: U.S. Government Printing Office. 2006. 182
25 White W B, Tai C K. Inferring interannual changes in global upper ocean heat storage from TOPEX altimetry. J Geophys Res [Oceans], 1995, 100: 24943–24954
26 Mccreary J P, Lu P. Interaction between the subtropical and equatorial ocean circulations—The subtropical cell. J Phys Oceanogr, 1994, 24: 466–497
27 Gu D F, Philander S G H. Interdecadal climate fluctuations that depend on exchanges between the tropics and extratropics. Science, 1997, 275: 805–807
28 Huang R X, Huang C J, Wang W. Dynamical roles of mixed layer in regulating the meridional mass/heat fluxes. J Geophys Res [Oceans], 2007, 112: C05036
29 Zhou T J, Yu Y Q, Liu H L, et al. Numerical simulation of the sensitivity of the Pacific subtropical-tropical meridional cell to global warming. Prog Nat Sci, 2006, 16: 507–511
30 Vecchi G A, Clement A, Soden B J. Examining the tropical Pacific's response to global warming. Eos Trans AGU, 2008, 89: 81–83
31 Dang H W, Jian Z M, Bassinot F, et al. Decoupled Holocene variability in surface and thermocline water temperatures of the Indo-Pacific warm pool. Geophys Res Lett, 2012, 39: L01701
32 Linsley B K, Rosenthal Y, Oppo D W. Holocene evolution of the Indonesian throughflow and the western Pacific warm pool. Nat Geosci, 2010, 3: 578–583
33 Stott L, Timmermann A, Thunell R. Southern hemisphere and deep-sea warming led deglacial atmospheric CO_2 rise and tropical warming. Science, 2007, 318: 435–438
34 Jiang L, Jian Z, Chen X. Oxygen and carbon stable isotopic records of planktonic foraminifers from the western equatorial Pacific since the Last Glacial Maximum (in Chinese). Mar Geol Quat Geol, 2004, 24: 67–71